A Low Cost, Low Speed Wind Tunnel For Dynamic Stall Measurement

A. Ruótolo, J. Meseguer
IDR/UPM
Escuela Técnica Superior de Ingenieros Aeronáuticos
Universidad Politécnica de Madrid
e-mail: andrea.ruotolo@upm.es
phone:+34 91 336 6353
fax: +34 91 336 6363

Summary

Aiming to improve the knowledge on both dynamic and static stall of airfoils for wind turbine applications, a new experimental facility (CCB6 wind tunnel) specifically devoted to this application has been developed. The design goals of this project have been to build up a low cost, low speed wind tunnel which can be easily adapted to a wide range of experimental specifications, whose test chamber, and even the whole geometry, can be modified at low cost. In this paper the main features of this new facility as well as the instrumentation involved are described. Besides, results of some preliminary tests concerning dynamic stall conducted on bodies with elliptical shape, when subjected to an oscillatory pitching motion, are presented.

1. Introduction

Typically the lifetime of wind turbine components is less than the standard 20-30 year design lifetime. These components, such as blades, hub and generators, are subjected to dynamic loads far in excess of their design loads. A primary source of these loads comes from the unsteady aerodynamic environment where wind turbines operate most of their life time.
Airfoil sections of wind turbine blades are subjected to large time dependent variations in angle of attack, the forces varying both in time and in space because of wind turbulence and shear, as well as blade oscillations, control inputs, and skewed flow. All these perturbations can lead to dynamic stall, an unsteady, non linear aerodynamic phenomenon also appearing in many other technical fields where lifting surfaces can reach angles of incidence far beyond the static stall angle. The discussion and reviews on this phenomenon have been well documented [1-4]. Traditionally, different approaches, such as experimentations [5-7], numerical simulations [8,9], and semi-empirical methods [10-14], have been widely employed to investigate this phenomenon.
In spite of the large amount of effort devoted to airfoil dynamic stall, this phenomenon is not completely understood. In addition, although many theoretical and numerical studies have been devoted to oscillating aerodynamic profiles, the availability of experimental results concerning the dynamic stall of airfoils for wind energy applications is still scarce.
Having in mind all the above limitations and drawbacks, the development of the CCB6 wind tunnel has been accomplished. Design specifications have been considered in order to develop a low cost, low speed wind tunnel with the appropriate instrumentation for dynamic stall tests. It must be pointed out that although this wind tunnel has been tailored to the volume constraints existing at IDR laboratories, because on its modular design it can be easily adapted to other rather different geometrical circumstances.
The facility is an open circuit wind tunnel in which a Reynolds number up to 10^6 can be achieved with an airfoil chord of 0.5 m. The wind tunnel geometry and performance, as well as its instrumentation are described, and some preliminary results are shown.

2. Methods

2.1. CCB6 facility

The CCB6 wind tunnel is an open circuit (Eiffel type) wind tunnel, 12 m in length and 3.3 m in height, which is place inside one of the laboratories of the IDR/UPM building of Montegancedo´s Campus. The room where this wind tunnel is mounted is specifically devoted to this facility, the room´s dimensions being 14.6 m in length, 5.2 m wide and 3.5 m height.

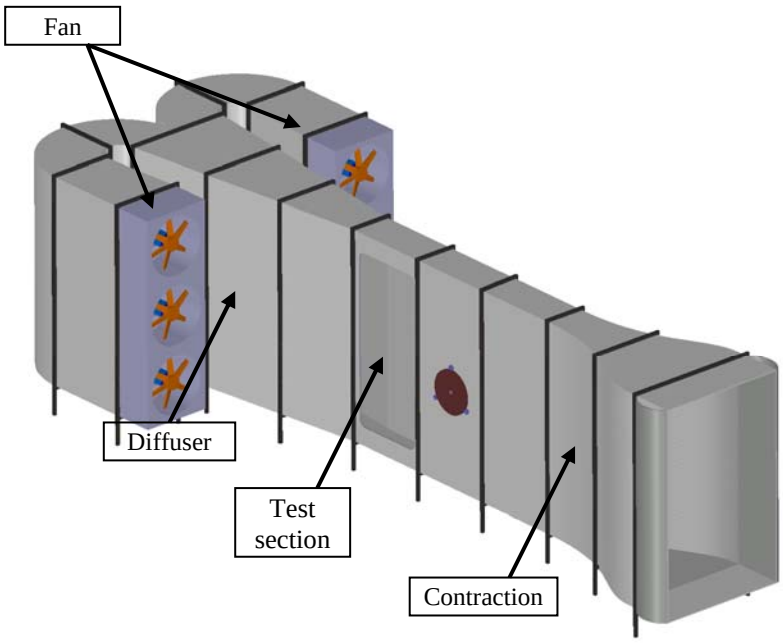

Figure 1. Sketch of the CCB6 wind tunnel with main components.

The support structure of the wind tunnel consists of 15 frames made of commercial steel with 40x40 mm square shaped that are anchored on the ground. The structure has been designed to withstand the static loads and vibrations.

The facility, as sketched in Figure 1, is arranged according to the traditional sequence of contraction, test chamber, diffuser and fans, the flow returning to the intake section through the room where the wind tunnel is located.

The contraction ratio is 4:1, and it is almost two-dimensional, as floor and ceiling are almost parallel; turbulence intensity at the test chamber is controlled through interchangeable mesh screens placed at the wind tunnel intake. Besides, although they are not yet implemented, some devices for gust generation, like turning vanes at the entrance of the test chamber, are foreseen.

The test chamber is closed, with a cross section of 0.54 m wide and 2.5 m height, the total length being 3.6 m. The models to be tested span between the lateral walls of the test chamber, all the stimuli devices as well as measurement instrumentation being located outside the test chamber. In normal operation the airfoil to be tested is anchored to a circular bar which can be rotated and vertically displaced as required. Under normal circumstances, to cover the normal operation range of a rotor blade, the angle of attack of a blade section can vary from $\alpha = -20^{o}$ to $\alpha = 30^{o}$.

For test specimens a normalized airfoil chord of 0.5 is selected, which assures a blockage of the test section less than 12% for angles of attack up to α = 30º.

The wind tunnel is equipped with six 7.5 kW fans, each of 0.9 m in diameter, arranged in two columns with three fans in each. Air velocity in the test section can be selected by controlling the fans frequency.

Floor and ceiling of the test section are equipped with 63 pressure taps each; there is also a pressure rake downstream of test section consisting of total pressure probes and static tubes. The distribution of the total pressure tubes in the rake is not uniform, the tube spacing being denser at the middle of the rake.

2.2. Experimental setup

Airfoil test specimens are mounted at 1.25 m from the tunnel floor and at 2 m from the test chamber inlet. Airfoils can be equipped with up to 63 pressure taps made of brass tube of 1 mm inner diameter located along the centreline.

The models are manufactured with Necuron 400, which is a low density easy machining plastic material; they are machined in two pieces (an upper and a lower shell) to facilitate instrumentation. To make pressure taps, holes are drilled on the airfoil surface and brass tubes are fitted to the holes and mounted flush with the surface. Flexible plastic tubes are connected at the ends of the brass tubes; the plastic tubes leave the airfoil through a hollow suspension axis, which is supported on by two bearings.

Dynamic stall has been experimentally studied mainly by using oscillating two dimensional aerofoils in wind tunnel tests. Most of the available results are dealing with airfoils oscillating in pitch (α). However, since the stall problem is highly non-linear the effect of other pertubations, either isolated or together, is important for reaching a better understanding of the phenomenon [15]. Because of these requirements, the experimental system developed at

IDR/UPM allows to perform static studies as well as dynamic ones, considering plunging and pitching motions, constant angular rate or ramp-type motion and time varying incident velocity or horizontal gusts. Other parameters involved, such as Reynolds number, and for each one of the imposed perturbation (rotation and translation) the mean value, reduced frequency, and amplitude, can be selected.

According to the above description, the standard instrumentation is

- Pressure taps on the upper and lower surfaces of airfoils, to measure the static pressure distribution, usually placed at the mid span plane.
- Pressure taps at the floor and ceiling of the test section to measure the static pressure distribution along the test chamber.
- A wake rake, downstream of the airfoil equipped with total and static pressure tubes to measure the vertical pressure distributions.
- Besides the mechanism responsible of airfoil motion provides information on vertical airfoil displacement and velocity as well as angle of attack and angular velocity. Other parameters under control are the electric AC frequency supplied to the fans as well as additional flow properties (air temperature and moisture and atmospheric pressure).
- There are also two Pitot tubes to measure static and total pressure at different locations in the test section, which are used to measure velocity, turbulence level and the stability of the flow at the working section.

One of the goals of the design is to obtain redundant results. In this way pressure distributions on the airfoils can be used to calculate the airfoil force coefficients, mainly lift and pitching moment coefficients, as well as the pressure drag coefficient (although this last force coefficient is only a reasonable approximation to total drag when the flow is separated).
The floor and ceiling longitudinal pressure distributions are used to calculate the lift coefficient by using the Betz method, whereas the total drag coefficient results from the wake rake total and static pressure distributions (these calculations are valid only when the airfoil flow is attached [16]).

- In addition, wind tunnel instrumentation includes hot wire and laser Doppler anemometry (also PIV anemometry is foreseen).

2.3. Data acquisition system

The data acquisition system, as shown in Figure 2, is two ZOC33 pressure-scanning modules from Scanivalve Corp. which record the pressure signals. A commercial data acquisition card from National Instruments Corp is used for the rest of the electrical signals.
The ZOC33 pressure scanning module consists of an electronic pressure scanner that accepts 64 pneumatic inputs which are directed to 64 silicon pressure sensors at a maximum 600 Hz sampling rate. Extensive experiments were conducted to ensure that the frequency response of the pressure-measuring system was kept well above the highest frequency to be measured. Each transducer data is collected via a terminal board and transformed to the computer through a 12-bit Analog-Digital (A/D) board. Raw data were then digitally filtered using a low-pass filtering routine. During the filtering process, cut off and transition frequencies were varied until the deviation between the original and the filtered data was minimum.

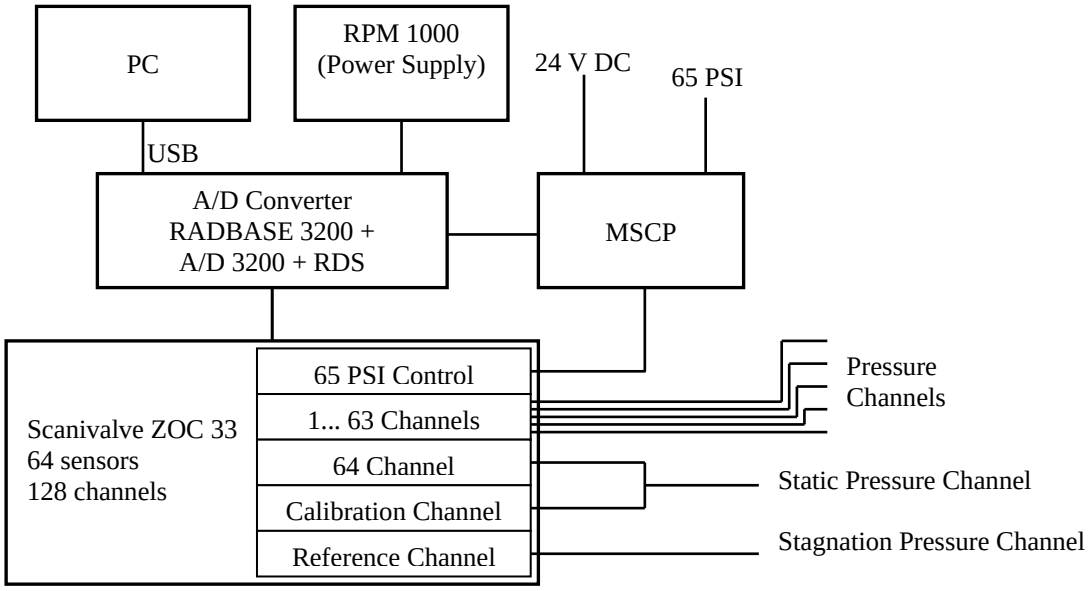

Figure 2. Block diagram of the pressure measurements system.

For controlling the Scanivalve, each module is equipped with a calibration valve, a high speed (50 kHz) multiplexer and an instrumentation amplifier (the MSCP modulus).
The calibration valve can be operated in four different modes that are operate, calibrate, purge and leak test. Applying the appropriate pneumatic control activates these modes. As a result the pressure modules can be calibrated/ checked during a measurement session.
As the silicon pressure sensors are known to be temperature dependent, the modules are placed inside thermal control units (TCU) which are designed to provide a constant temperature environment for the pressure scanners while being equipped with electrical and pneumatic connections, thus functioning as an intermediate between the ZOC and the rest of the system.

3. Results

Some preliminary tests with bodies having elliptical shape have been performed; the bodies being subjected to steady and an oscillatory pitching motion.
All measurements series contained measurements from airfoil pressure. Two different models have been used, having different relative thickness τ, both are elliptical in shape, one of them with τ=0.21 and the second with τ=0.49 at Re = 8×10^5.
Two different types of test have been made:

- Steady test at α of ±24º, ±36º and ±46º.
- Dynamic measurement in pitching movement around the symmetry axis with an amplitude of oscillation of ±24º, ±36º and ±46º at 2.4 Hz.

Figure 3 shows the pressure tap location of both models in the centre region along the chord.

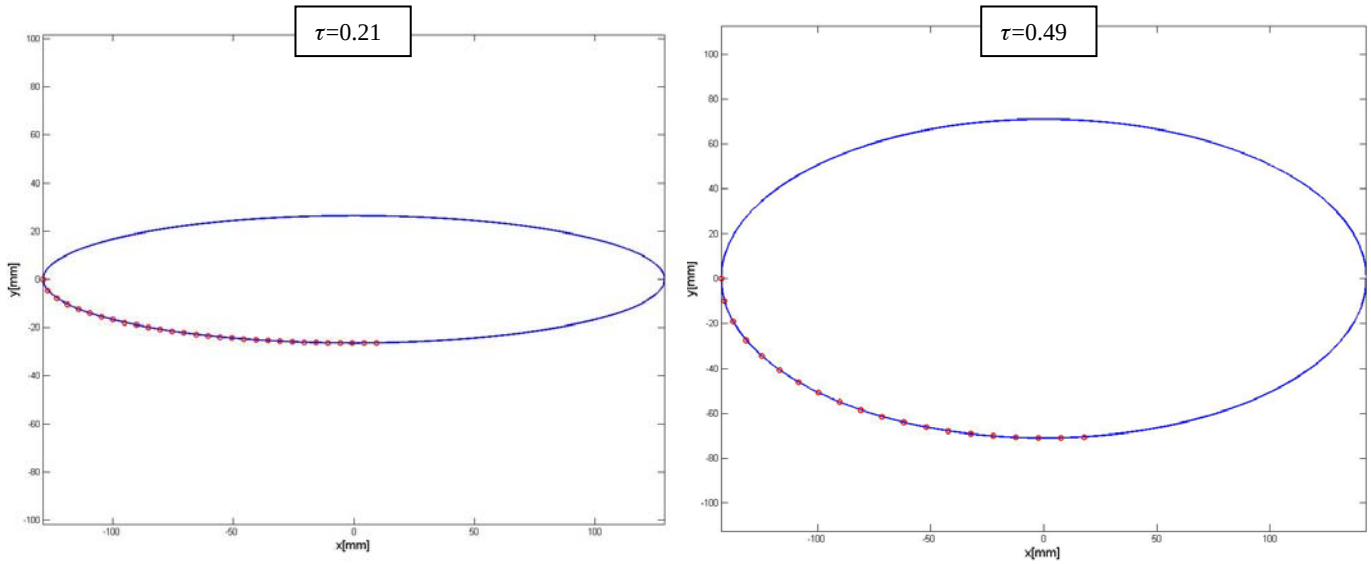

Figure 3. Pressure taps (dots) location of the different airfoil models (line) in the centre region along the chord.

The steady (blue dots) and dynamic (red line) results at different pressure tap locations along the τ=0.21 chord model are shown in Figures 4 to 6. Experimental results correspond to pressure taps located at *x*/*c*= 0.46, 0.25 and 0.06 respectively. These results are the average values of $N_{samples}$ =1800 (number of samples) at a sampling rate of 200Hz.
From the static results, in the case α is -24º, the airfoil has a suction peak at *x*/*c*= 0.46. For higher *x*/*c* ratios, c_p becomes uniform due to the fact that the airfoil is under stall.
As α decreases, specifically when the angle of attack is -36º and -46º, the airfoil stalls and separation removes the suction peak and the suction side pressure becomes nearly uniform.
Comparing the static and dynamic results at *x*/*c*= 0.46, there exists a delay of the stagnation point appearing. For *x*/*c*= 0.25 and 0.06 there is no stagnation point at any α.

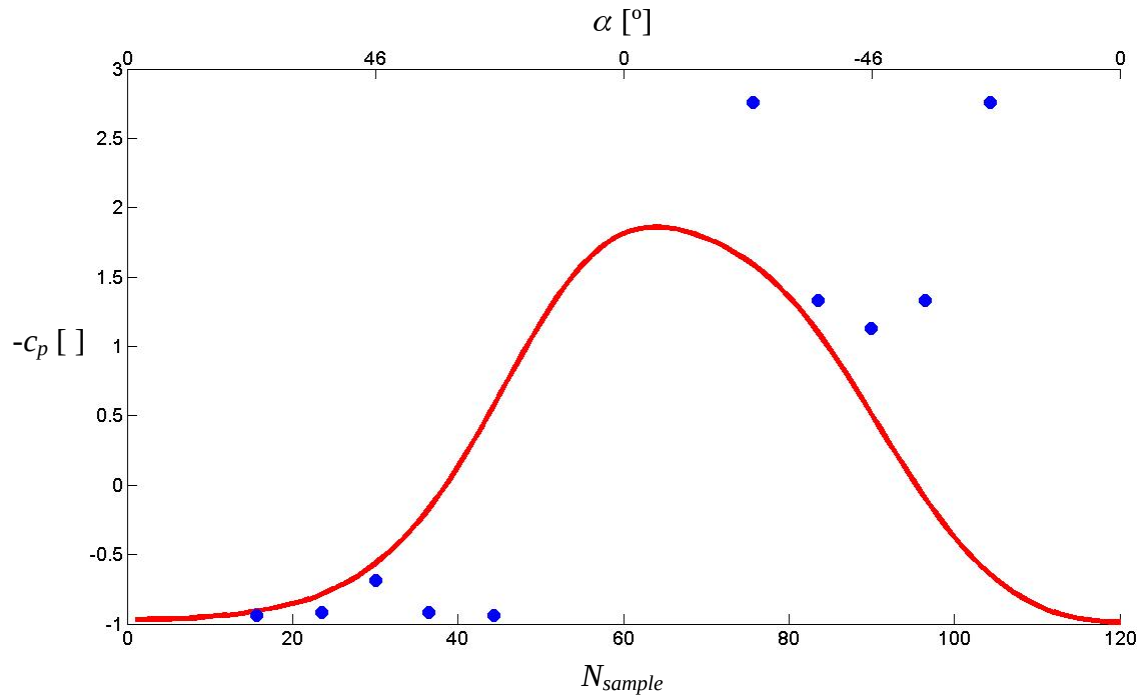

Figure 4. Pressure coefficient, c_p, versus angle of attack α, measured at the pressure tap located at *x/c*= 0.46 under steady test conditions (blue dots) at α= ±24º, ±36º and ±46º and dynamic oscillation (red line) with ±46º amplitude. Results correspond to the airfoil with τ=0.21.

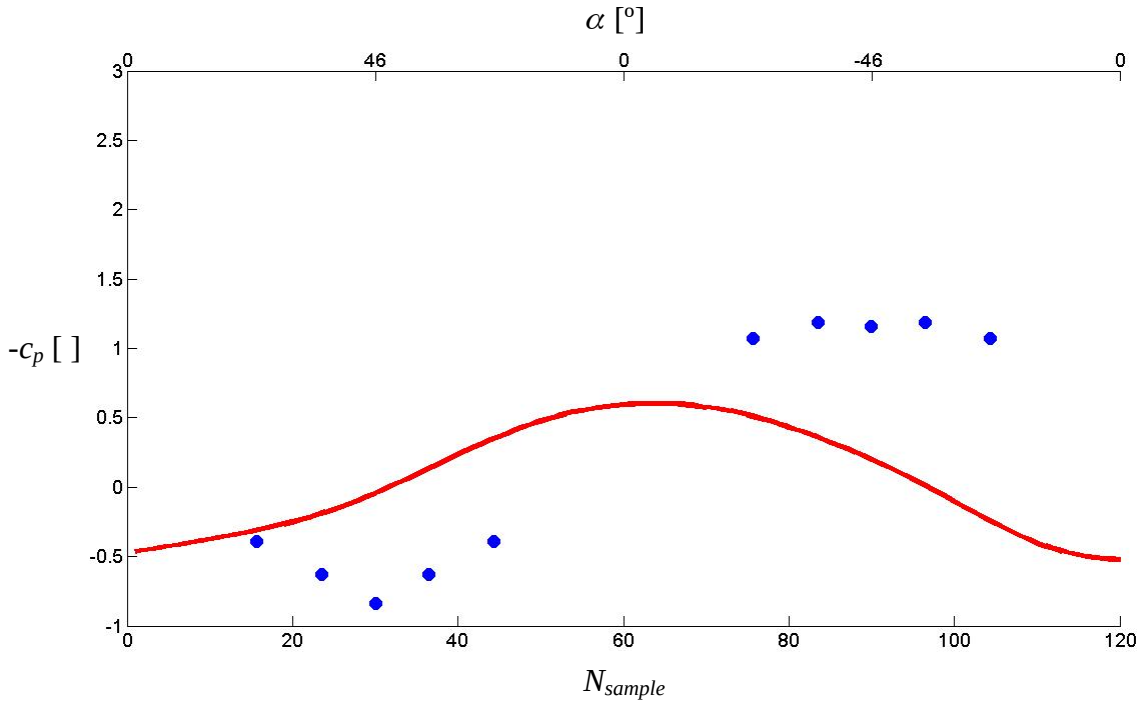

Figure 5. Pressure coefficient, c_p, versus angle of attack α, measured at the pressure tap located at *x/c*= 0.25 under steady test conditions (blue dots) at α= ±24º, ±36º and ±46º and dynamic oscillation (red line) with ±46º amplitude. Results correspond to the airfoil with τ=0.21.

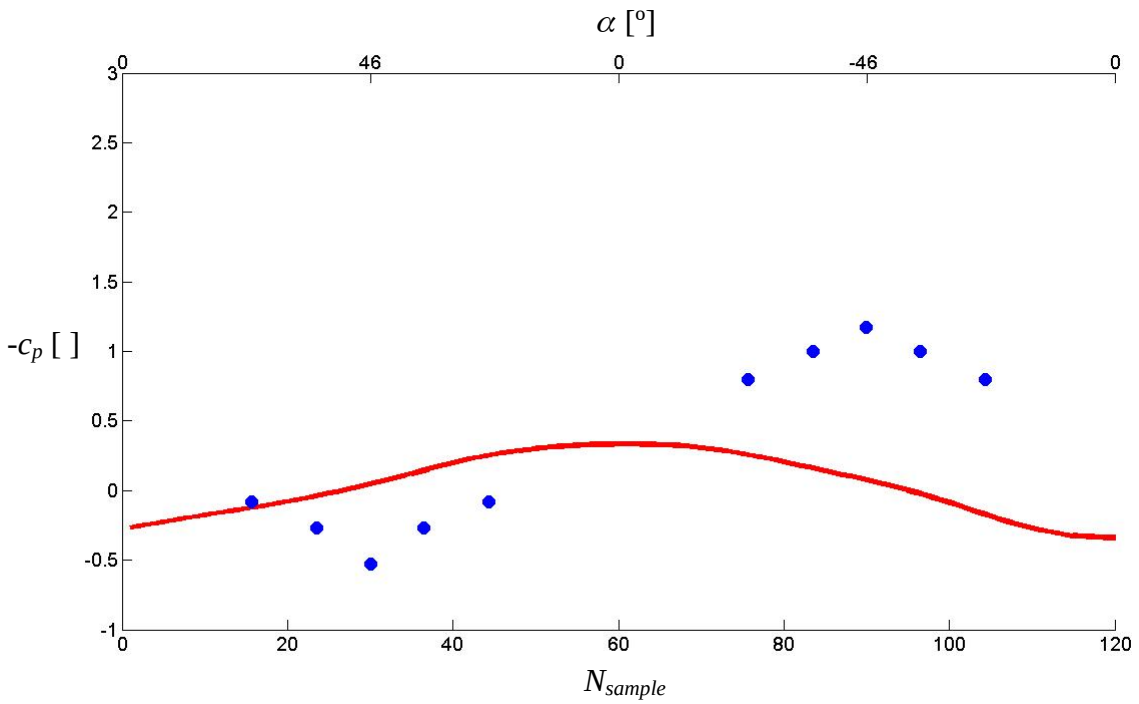

Figure 6. Pressure coefficient, c_p, versus angle of attack α, measured at the pressure tap located at *x/c*= 0.06 under steady test conditions (blue dots) at α= ±24º, ±36º and ±46º and dynamic oscillation (red line) with ±46º amplitude. Results correspond to the airfoil with τ=0.21.

Figure 7 shows the steady (blue dots) and dynamic (red line) results that correspond to the pressure tap located at *x/c*= 0.46 along the τ=0.49 chord model.

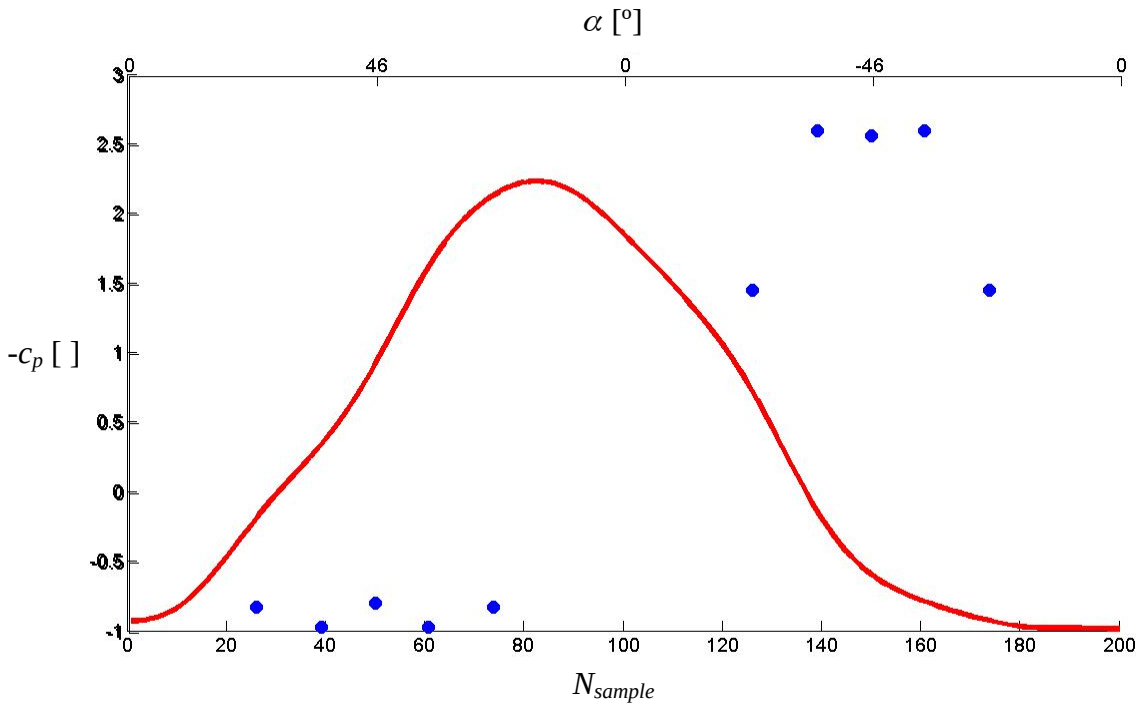

Figure 7. Pressure coefficient, c_p, versus angle of attack α, measured at the pressure tap located at *x/c*= 0.46 under steady test conditions (blue dots) at α= ±24º, ±36º and ±46º and dynamic oscillation (red line) with ±46º amplitude. Results correspond to the airfoil with τ=0.49.

As in the case of model τ=0.21, for the different amplitudes it can be observed that the stagnation zone is always located in the first 5% of the chord, and the delay in the appearing of the stagnation point.

4. Conclusions

A low cost, low speed two-dimensional testing facility was designed to fulfill the requirements of dynamic stall experimentation. The experimental system developed at IDR/UPM allows to perform static studies as well as dynamic ones, considering plunging and pitching motions, constant angular rate or ramp-type motion and time varying incident velocity or horizontal gusts. Other parameters involved, such as Reynolds number, and for each one of the imposed perturbation (rotation and translation) the mean value, reduced frequency, and amplitude, can be selected.

Preliminary steady and dynamic tests were carried out to study the response of the measurement and acquisition system. Measurements of the pressure distribution around two different models, both elliptical in shape, having different relative thickness τ, have been made. The steady and dynamic (oscillatory pitching motion) results showed that the developed wind tunnel is in agreement with imposed requirements.

References

1. Carr LW. Progress in Analysis and Prediction of Dynamic Stall. *J. Aircraft* 1988; 6-17.
2. Carr LW, Chandrasekhara, MS. Compressibility Effects on Dynamic Stall. *Prog. Aerosp. Sci.* 1996; 523-573.
3. Ekaterinaris JA, Platzer MF. Computational Prediction of Airfoil Dynamic Stall. *Prog. Aerosp. Sci.* 1997; 759-846.
4. McCroskey WJ, McAlister KW, Carr LW, Pucci SL, Lambert O, Indergrand RF. Dynamic Stall on Advanced Airfoil Sections. *J.Am. Helicopter Soc.* 1981; 40-50.
5. McAlister KW, Carr LW, McCroskey WJ. Dynamic Stall Experiments on the NACA 0012 Airfoil. *NASA, Technical Paper* 1978; No. 1100.
6. McCroskey WJ. Dynamic Stall Experiments on Oscillating Airfoils. *AIAA J.* 1976; 57-63.
7. Lee T, Gerontakos P. Investigation of Flow Over an Oscillating Airfoil. *J. Fluid Mech.* 2004; 313-341.
8. Guilmineau E, Queutey P. Numerical Study of Dynamic Stall on Several Airfoil Sections. *AIAA J.* 1999; 128-130.
9. Spentzos A, Barakos GN, Badcock KJ, Richards BE, Wernert P, Schreck S, Raffel M. Investigation of Three-Dimensional Dynamic Stall Using Computational Fluid Dynamics. *AIAA J.* 2005; 1023-1033.
10. Beddoes TS. Onset of Leading Edge Separation Effects Under Dynamic Conditions and Low Mach Number. *34th Annual National Forum of the American Helicopter Society* 1978.
11. Beddoes TS. Practical Computational of Unsteady Lift. *Vertica* 1984; 55-71.
12. Leishman JG, Beddoes TS. A Semi-Empirical Model for Dynamic Stall. *J. Am. Helicopter Soc.* 1989; 3-17.
13. Beddoes TS. A Third Generation Model for Unsteady Aerodynamic and Dynamic Stall. Westland *Helicopter Limited* 1993. Report No. RP-908.
14. Sheng W, Galbraith RA McD, Coton FN. A New Stall-Onset Criterion for Low Speed Dynamic-Stall. *ASME J. Sol. Energy Eng.* 2006; 461-471.
15. Leishmann JG. Challenges in Modelling the Unsteady Aerodynamics of Wind Turbines. *J. Wind Energy* 2002; 85-132.
16. Fugsland P, Bove S. Wind Tunnel Testing Of Airfoils Involves More Than Just Wall Corrections.*European Wind Energy Conference* 2008.